Molecular tweezers inhibit islet amyloid polypeptide assembly and toxicity by a new mechanism

Dahabada H. J. Lopes[1], Aida Attar[1,2], Gayatri Nair[1], Eric Hayden[1,] Zhenming Du[4], Kirsten McDaniel[1], Som Dutt[5], Kenny Bravo-Rodriguez[6], Sumit Mittal[6], Frank-Gerrit Klärner[5], Chunyu Wang[4], Elsa Sanchez-Garcia[6], Thomas Schrader[5], and Gal Bitan[1,2,3*]

[1]Department of Neurology, David Geffen School of Medicine, [2]Brain Research Institute, and [3]Molecular Biology Institute, University of California at Los Angeles, Los Angeles, CA; [4]Department of Biology, Rensselaer Polytechnic Institute, Troy, NY; [5]Institute of Organic Chemistry, University of Duisburg-Essen, Essen, Germany; [6]Max-Planck-Institut für Kohlenforschung, Mülheim an der Ruhr, Germany

SUPPLEMENTARY INFORMATION

Supplementary Methods

Synthesis of IAPP fragments. IAPP fragments were synthesized on a CEM Liberty Microwave Peptide Synthesizer using 9-fluorenylmethoxycarbonyl (FMOC) chemistry according to standard protocols on FMOC-Rink amide MBHA resin. Protected amino acids were activated with 2-(6-Chloro-1H-benzotriazole-1-yl)-1,1,3,3-tetramethylaminium hexafluorophosphate in the presence of N,N-diisopropylethylamine in 1-methyl-2-pyrrolidinone and the FMOC group was deprotected with piperidine. Cysteine, arginine, and leucine were always coupled twice. Peptides were cleaved off the resin using a cold mixture of 95% trifluoroacetic acid (TFA), 2.5% triisopropylsilane, and 2.5% water and subsequently precipitated with cold diethyl ether. The intramolecular disulfide bridge formed by subsequent mild oxidation or *in situ* by carrying out the peptide synthesis in air (high-resolution mass-spectrometry evidence). Peptide purity was monitored by RP-HPLC using water and

acetonitrile gradient containing 0.1% TFA. $IAPP_{1–14}$: yield 60%, purity 97.4%; $IAPP_{2–14}$: yield 89%, purity 93.0%; $IAPP_{1–7}$: yield 87%, purity 91.0%; $IAPP_{2–7}$: yield 85%, purity 90.0%.

Disaggregation Experiment:

ThT fluorescence assay. IAPP was prepared in phosphate buffer (PB) and aliquoted into 96-well plates at 10-μM final concentration. Each well also contained 30 μM ThT. The final volume in each well was 200 μl. The reactions were incubated at 25 ºC without shaking and fluorescence was monitored with λ_{ex} = 420 nm and λ_{em} = 485. Ten-fold CLR01 were added at 7 h or 170 h and the reactions were monitored up to 500 h. Ten-μl aliquots of the reaction mixtures were removed periodically for morphological examination by EM. The data are presented as means ± SEM of 1–3 independent experiments with at 3–10 replicates each.

Electron microscopy (EM). Ten μM aliquots of the reaction mixtures from the ThT fluorescence assay were spotted on glow-discharged, carbon-coated Formvar grids (Electron Microscopy Science) and stained with 1% uranyl acetate as described previously (*1*). The samples were analyzed using a JEM1200-EX (JOEL) transmission electron microscope. Fibril diameter and length, and oligomer diameter were measured using ImageJ (available at http://rsb.info.nih.gov/ij). At least 20 measurements of each parameter were performed in each reaction at the time points indicated.

MTT assay. Cell viability was measured using the 3-(4,5-dimethylthiazol-2-yl)-2,5-diphenyltetrazolium bromide (MTT) reduction assay in rat insulinoma (RIN5fm) cells as described previously (*2*). Briefly, cells were treated for 24 h with $IAPP_{1–37}$ or $IAPP_{2–37}$ in the absence or presence of MTs and cell viability was assessed using a Promega CellTiter 96 kit. At least three independent experiments with six replicates ($n \geq 18$) were carried out and the results were averaged and presented as mean ± SEM.

NMR of IAPP fragments. Experiments examining the interaction between CLR01 and unlabeled IAPP fragments were carried out at 25 °C using a Bruker DRX-500 MHz

spectrometer equipped with a 5-mm QNP-Probe (^{1}H) or a 5-mm TBI-Probe (^{1}H, X, ^{13}C) with Z-Gradient (gs-COSY90). ^{1}H-NMR of CLR01 alone was measured by dissolving CLR01 at 1 mM in 10 mM phosphate-buffered D_2O, pH 7.2. Solutions of IAPP fragments in the absence or presence of 1 or 3 equivalents of CLR01 were prepared in 10 mM sodium phosphate in 9:1 – H_2O:D_2O, pH 7.2, at peptide concentration of 1 mM in all cases. ^{1}H-NMR was measured with water suppression using presaturation and composite pulses (zgcppr). For COSY experiments, peptide samples were prepared in phosphate-buffered D_2O, pH 7.2, in the absence or presence of 1 or 3 equivalents of CLR01 and gs-COSY90 (cosygpqf) spectra were measured.

Fluorescence Titration. CLR01 was dissolved in 10 mM PB, pH 7.6, at 26 μM. The same CLR01 concentration was maintained in all IAPP solutions to keep the CLR01 concentration constant over the entire titration. Seven-hundred μl CLR01 were placed in a quartz cuvette of 1-cm path length and fluorescence spectra were measured on a JASCO FP-6500 spectrophotometer. Aliquots of peptide solution (increasing the concentration from 0.25 to 9 eq.) were added to the tube and fluorescence spectra were recorded following each addition. Binding isotherms for a 1:1 complex were obtained from fluorescence emission intensities at 336 nm and converted into binding constants by standard, non-linear regression fitting using Systat SigmaPlot 10.0.

Supplementary Results

CLR01 attenuates IAPP aggregation into β-sheet-rich fibrils at very low concentration ratios.

Using ThT measurements, we observed lower final ThT fluorescence, and primarily amorphous morphology by IAPP in the presence of CLR01 concentrations as low as 1 fM, relative to IAPP alone (Supplementary Figure S1A). The final ThT fluorescence at IAPP:CLR01 concentration ratio $1:10^{-10}$ was 69±2 % that of IAPP alone. The initial CD

spectrum of IAPP in the presence of 1 fM CLR01 was similar to that of IAPP in the presence of 10 nM CLR01 and development of β-sheet was attenuated relative to IAPP incubated in the absence of CLR01 (Supplementary Figure S1B). The morphology of IAPP in the presence of 1 fM CLR01 was predominantly amorphous, with occasional observation of thin, thread-like structures (Supplementary Figure S1C). Following 24 h of incubation, larger structures were observed but not amyloid fibrils. The basis for the effect of CLR01 on IAPP aggregation at such a low concentration (10 orders of magnitude lower concentration of CLR01 than IAPP) is not clear and will require additional investigation.

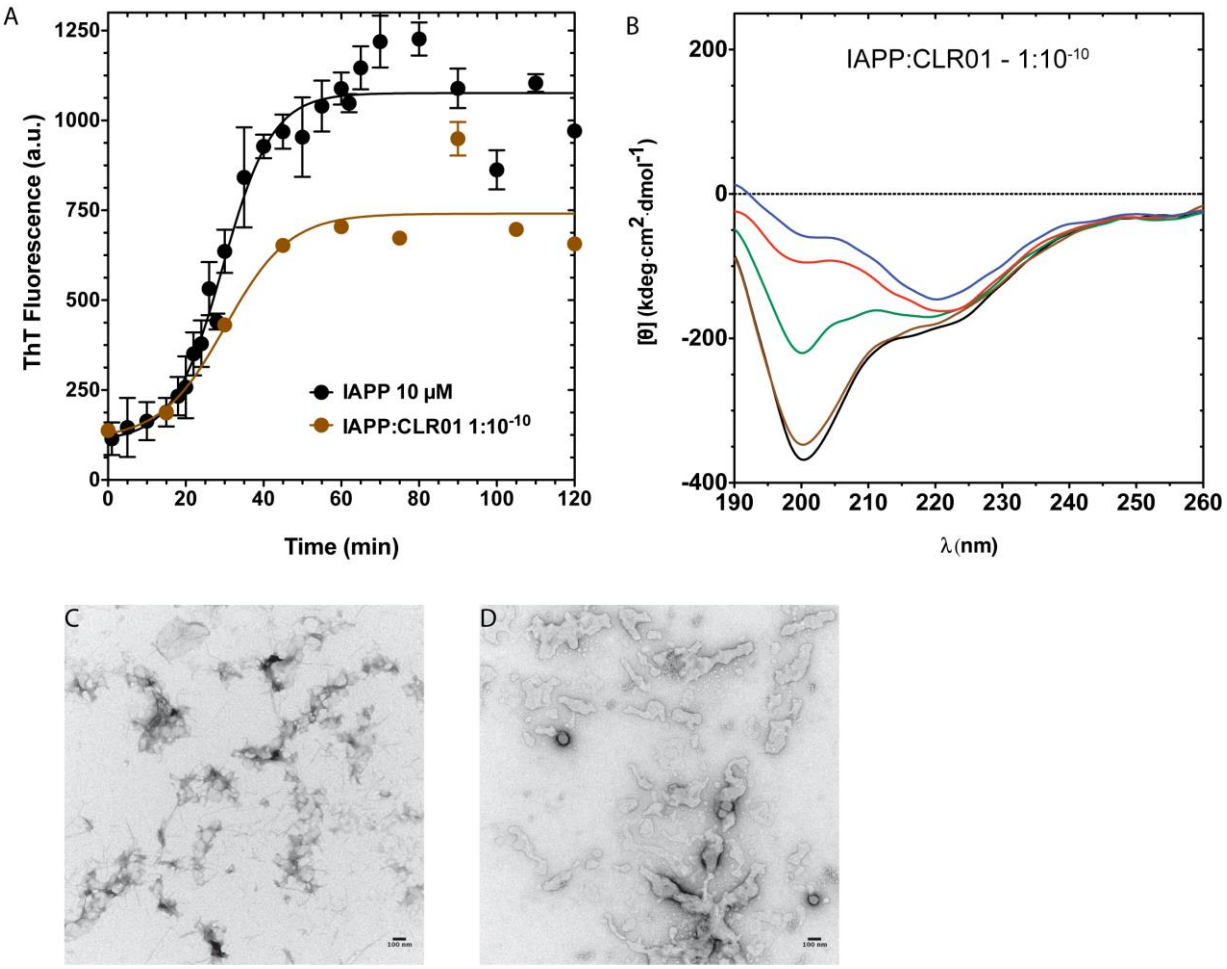

Supplementary Figure S1. CLR01 attenuates IAPP aggregation and β-sheet formation at concentrations as low as 1 fM. A) Ten μM IAPP were incubated in the absence or presence

of 1 fM CLR01 at 25 ºC with constant agitation and formation of β-sheet was measured using the ThT fluorescence assay. The data are presented as mean ± SEM of 3 independent experiments. B) Ten μM IAPP were incubated in the absence or presence of CLR01 or CLR03 at 25 ºC with constant agitation in 1-mm path length quartz cuvettes and CD spectra were recorded at the indicated time points. The spectra are representative of 4 independent experiments. C and D) Aliquots were taken at t = 0 (C) or 24 (D) h and examined by EM. The images are representative of 3 independent experiments. Scale bars denote 100 nm.

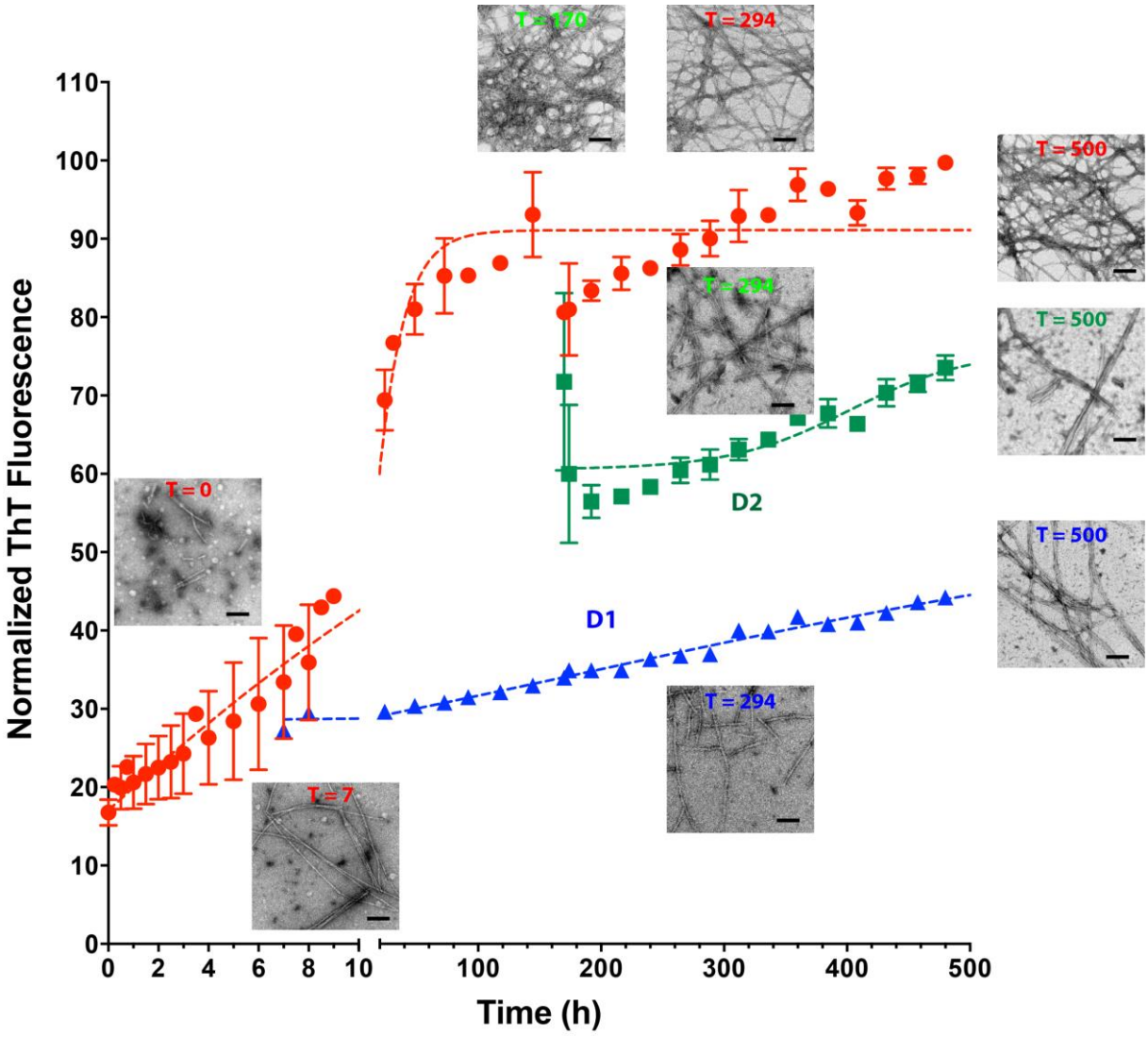

Time (h)		Control	D1	D2
0	Fibril Diameter (nm)	8.7 ± 1.5		
	Fibril Length (nm)	96 ± 51		

	Oligomer diameter (nm)	19 ± 5		
7	Fibril Diameter (nm)	7.8 ± 1.4		
	Fibril Length (nm)	343 ± 271		
	Oligomer diameter (nm)	22 ± 5		
170	Fibril Diameter (nm)	7.3 ± 1.3		
	Fibril Length (nm)	Indefinite		
294	Fibril Diameter (nm)	8.1 ± 1.9	9.1 ± 1.8	8.6 ± 1.1
	Fibril Length (nm)	Indefinite	148 ± 82	n.d.
500	Fibril Diameter (nm)	7.2 ± 1.4	9.0 ± 1.8	7.8 ± 1.4
	Fibril Length (nm)	Indefinite	316 ± 117	157 ± 83

Supplementary Figure S2. CLR01 halts IAPP aggregation. Ten μM IAPP were incubated in 96-well plates in the presence of 30 μM ThT without agitation at 25 ºC and monitored periodically for ThT fluorescence. Ten-fold excess CLR01 was added to one third of the wells after 7 h (D1) and to a second third of the wells after 170 h. The reactions were monitored up to 500 h. The data were normalized to the highest ThT fluorescence of IAPP alone and are presented mean ± SEM of 1–3 independent experiments with at least 3 wells per condition. Periodically, aliquots of the three reactions were taken for EM imaging. Scale bars represent 100 nm.

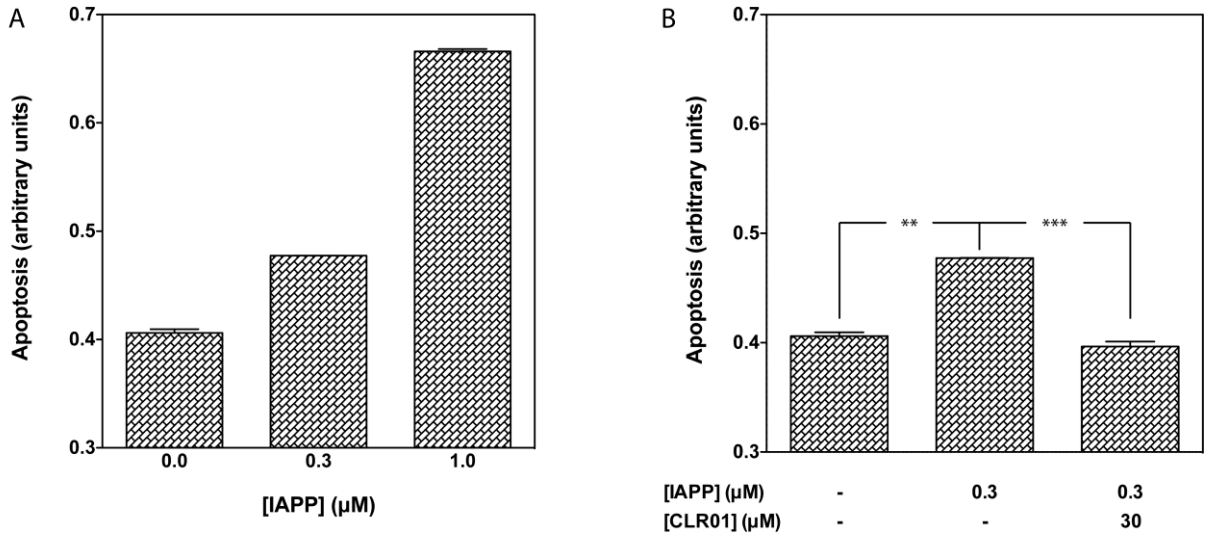

Supplementary Figure S3. CLR01 inhibits IAPP-induced apoptosis. A) IAPP was incubated at 0.3 or 1 μM with RIN5fm cells for 16 h. B) IAPP was incubated at 0.3 μM in the absence or presence of 30 μM CLR01 with RIN5fm cells for 16 h. Apoptosis was measured using a commercial ELISA kit for detection of cytoplasmic histone-associated nucleosomes. The data are shown as mean ± SEM of 2 independent experiments. Statistical analysis was done by 1-way ANOVA with *post hoc* Tuckey test. $^{**}p<0.01$, $^{***}p<0.001$.

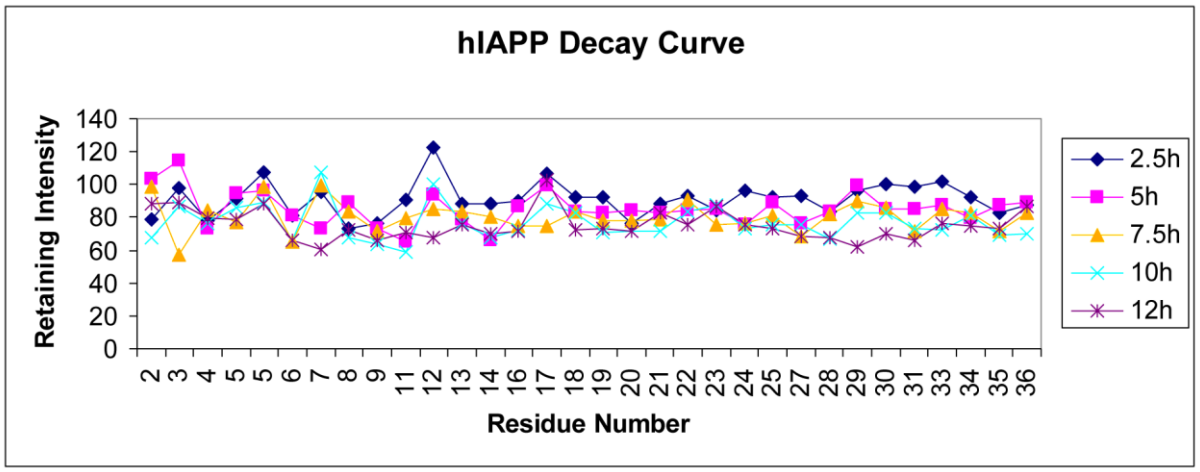

Supplementary Figure S4. The ^{1}H-^{15}N HSQC NMR signal of IAPP is stable for 12 h. One-hundred μM IAPP were incubated at 4 ºC and the ^{1}H-^{15}N HSQC NMR signal recorded at the indicated times.

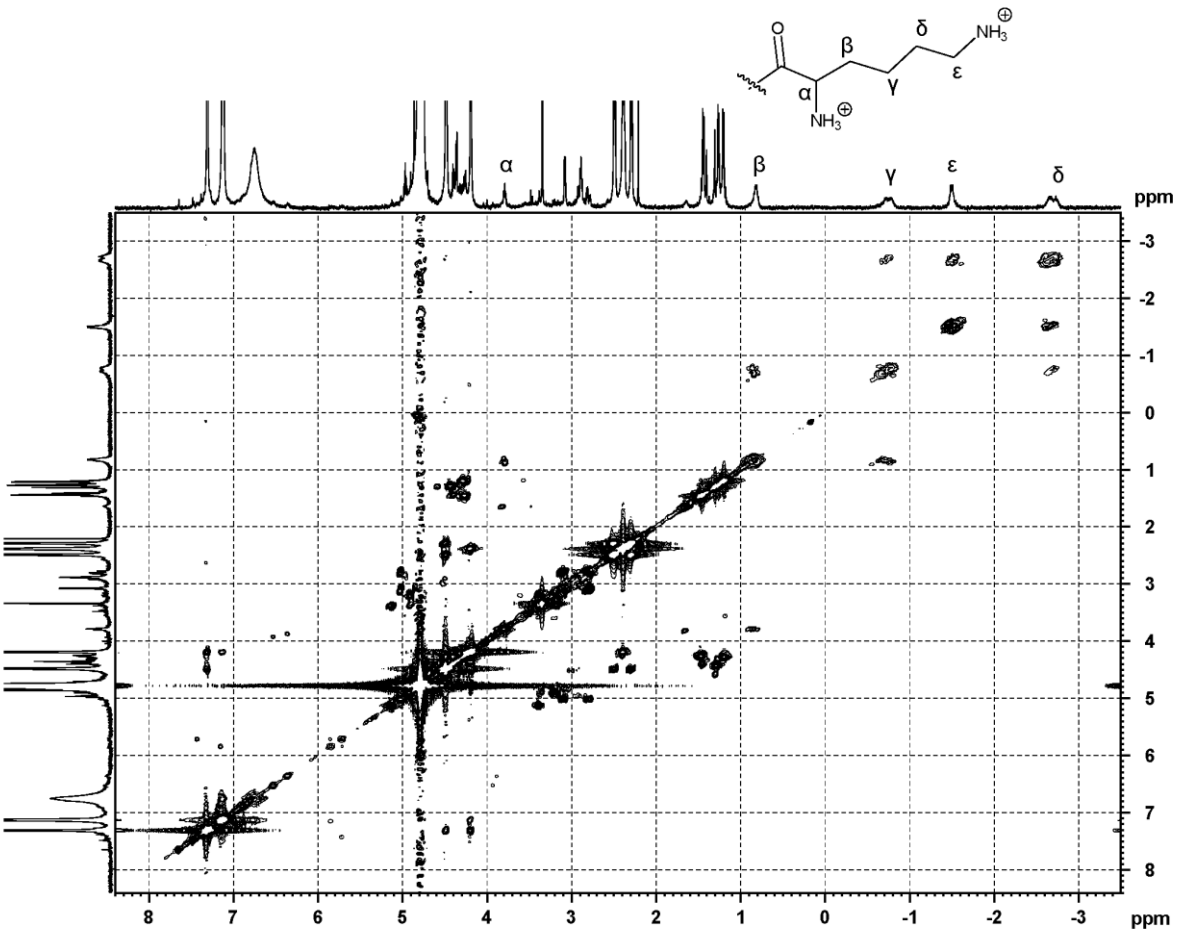

Supplementary Figure S5. gs-H,H-COSY NMR of 3:1 molar ratio of CLR01:IAPP$_{1-7}$, respectively, in D_2O phosphate buffer. K1 side chain protons in the complex are assigned as α, β, γ, δ, and ε.

Supplementary Figure S6. Fluorescence Titration of CLR01 with $IAPP_{1-7}$ in 10 mM sodium phosphate, pH 7.6.

λ_{ex} = 285 nm λ_{em} = 334 nm	Receptor CLR01	Guest $IAPP_{1-7}$
Amount [mg]:	0.225	0.263
Volume [mL]:	10.710	0.780
Concentration [M]:	2.579×10^{-05}	4.573×10^{-04}

Guest V (µL)	Receptor V (µL)	[Receptor] (M)	[Guest] (M)	[Guest]/ [Receptor]	F.I. ($I_{334\ nm}$)	ΔI_{obs}	ΔI_{calc}
0	700	2,58E-05	0,00E+00	0,00	612,158	0,000	0,000
10	710	2,58E-05	6,44E-06	0,25	569,172	42,986	47,290
20	720	2,58E-05	1,27E-05	0,49	530,430	81,728	87,553
30	730	2,58E-05	1,88E-05	0,73	492,028	120,130	120,483
40	740	2,58E-05	2,47E-05	0,96	463,046	149,112	146,461
60	760	2,58E-05	3,61E-05	1,40	427,225	184,933	181,757
80	780	2,58E-05	4,69E-05	1,82	409,022	203,136	202,571
100	800	2,58E-05	5,72E-05	2,22	396,970	215,188	215,482
140	840	2,58E-05	7,62E-05	2,95	383,541	228,617	230,017
180	880	2,58E-05	9,35E-05	3,63	375,852	236,306	237,774
240	940	2,58E-05	1,17E-04	4,53	367,371	244,787	244,284
300	1000	2,58E-05	1,37E-04	5,32	362,955	249,203	248,044

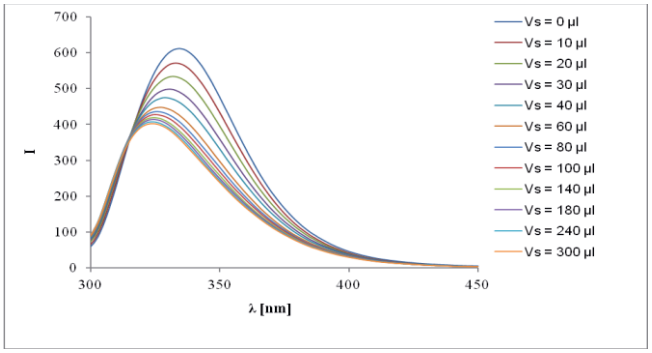

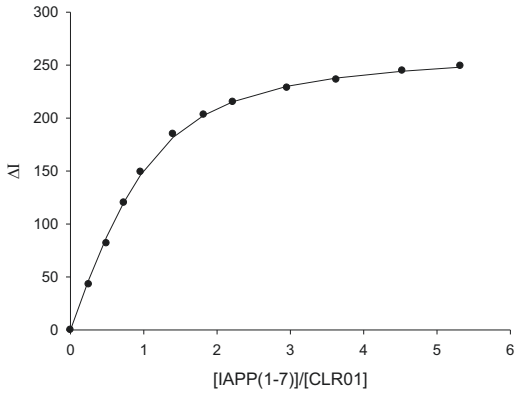

K_a [M^{-1}] = 115000 ± 6940 (± 6.0 %)
K_d = 8.69 µM

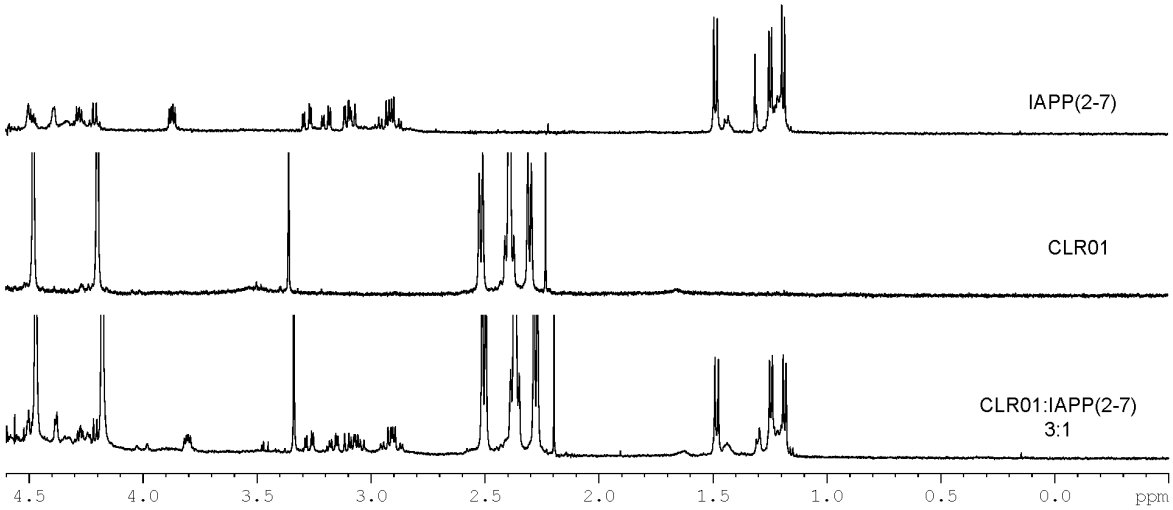

Supplementary Figure S7. ^{1}H-NMR spectra of 1.0 mM $IAPP_{2–7}$, 3.0 mM CLR01, and a 1:3 mixture of the two in 10 mM sodium phosphate, pH 7.2. No interaction is seen between CLR01 and peptide fragment.

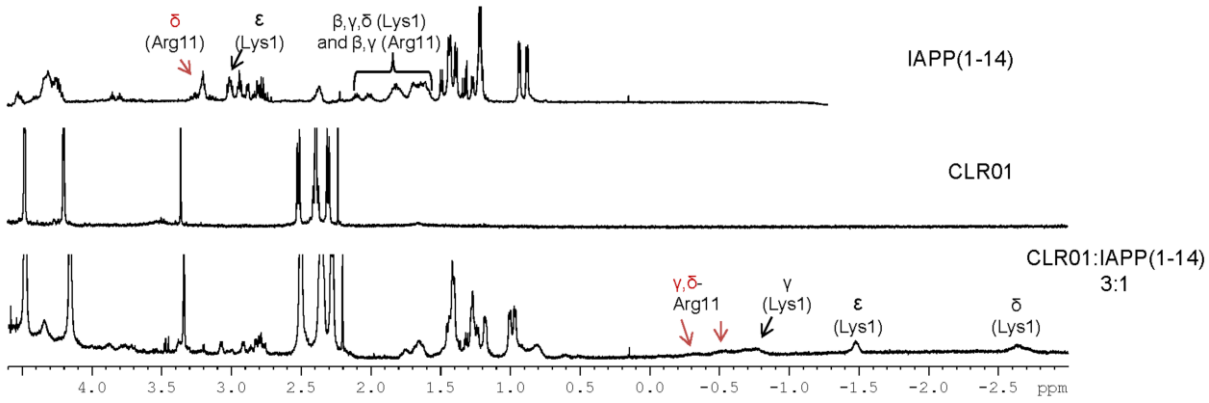

Supplementary Figure S8. ^{1}H-NMR spectra of 1.0 mM $IAPP_{1–14}$, 3.0 mM CLR01, and a 1:3 mixture of the two in 10 mM sodium phosphate, pH 7.2. CLR01 is involved in complex formation with both, K1 and R11 (K1 signals marked in black, R11 signals in red). Complexed K1 signals show almost the same upfield shift as in the complex with $IAPP_{1-7}$. By contrast, R11 signals are broadened and significantly less upfield-shifted than in the complex with $IAPP_{2-14}$ (Figure 6B), indicating, that CLR01 prefers K1 over R11.

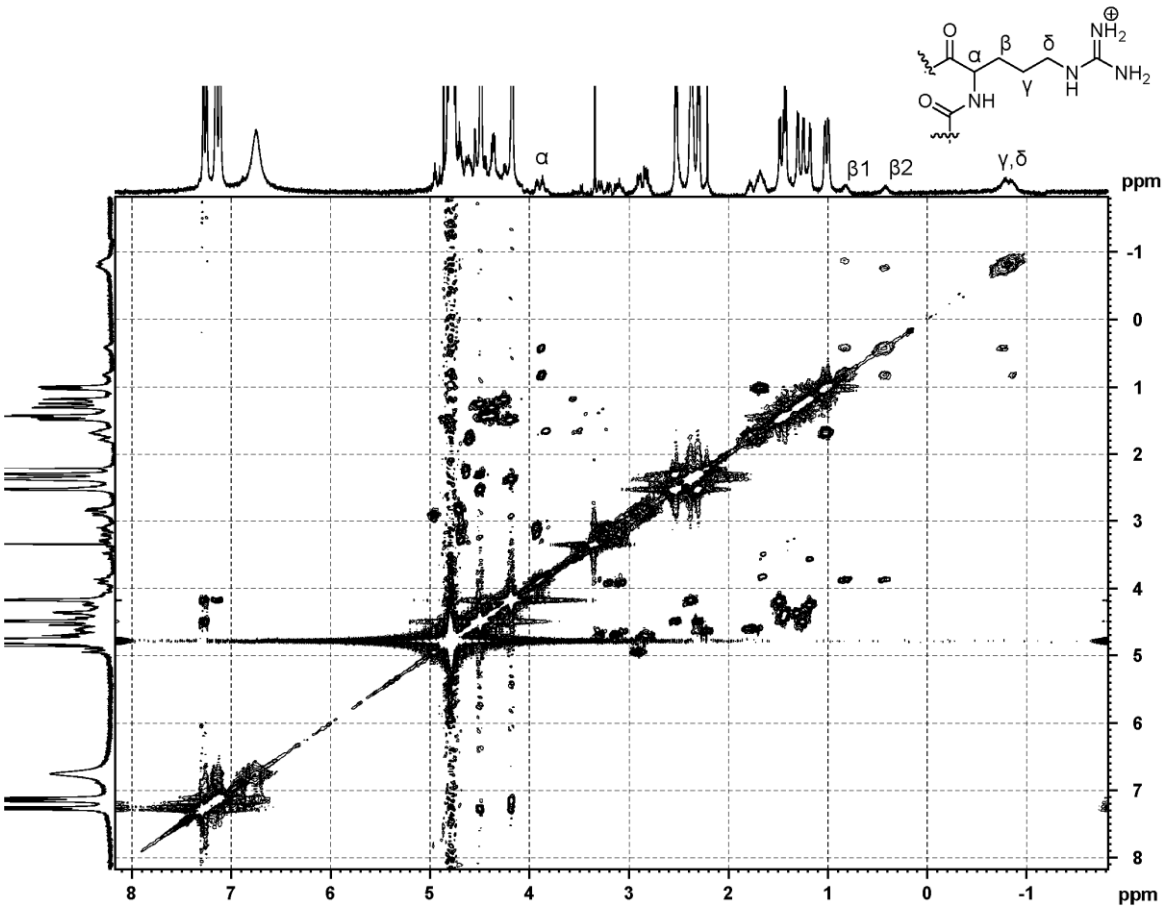

Supplementary Figure S9. **gs-H,H-COSY NMR of 3:1 molar ratio of CLR01:IAPP$_{2–14}$, respectively, in D_2O phosphate buffer.** R11 protons in the complex are assigned α, β, γ, and δ.

Supplementary Figure S10. Fluorescence Titration of CLR01 with $IAPP_{2–14}$ in 10 mM sodium phosphate, pH 7.6

λ_{ex} = 285 nm λ_{em} = 334 nm	Receptor CLR01	Guest $IAPP_{2-14}$
Amount [mg]:	0.225	0.549
Volume [mL]:	10.710	0.880
Concentration [M]:	2.579×10^{-05}	4.575×10^{-04}

Guest V (µL)	Receptor V (µL)	[Receptor] (M)	[Guest] (M)	[Guest]/ [Receptor]	F.I. ($I_{334\ nm}$)	ΔI_{obs}	ΔI_{calc}
0	700	2,58E-05	0,00E+00	0,00	596,576	0,000	0,000
10	710	2,58E-05	6,44E-06	0,25	580,210	16,366	17,418
20	720	2,58E-05	1,27E-05	0,49	564,679	31,897	33,094
30	730	2,58E-05	1,88E-05	0,73	553,575	43,001	47,254
40	740	2,58E-05	2,47E-05	0,96	537,644	58,932	60,086
60	760	2,58E-05	3,61E-05	1,40	510,046	86,530	82,404
80	780	2,58E-05	4,69E-05	1,82	496,676	99,900	101,094
100	800	2,58E-05	5,72E-05	2,22	481,567	115,009	116,932
140	840	2,58E-05	7,63E-05	2,96	450,962	145,614	142,223
180	880	2,58E-05	9,36E-05	3,63	434,443	162,133	161,446
240	940	2,58E-05	1,17E-04	4,53	412,349	184,227	182,862
300	1000	2,58E-05	1,37E-04	5,32	398,538	198,038	198,498
400	1100	2,58E-05	1,66E-04	6,45	382,369	214,207	216,847
600	1300	2,58E-05	2,11E-04	8,19	359,076	237,500	238,599
700	1400	2,58E-05	2,29E-04	8,87	349,319	247,257	245,559

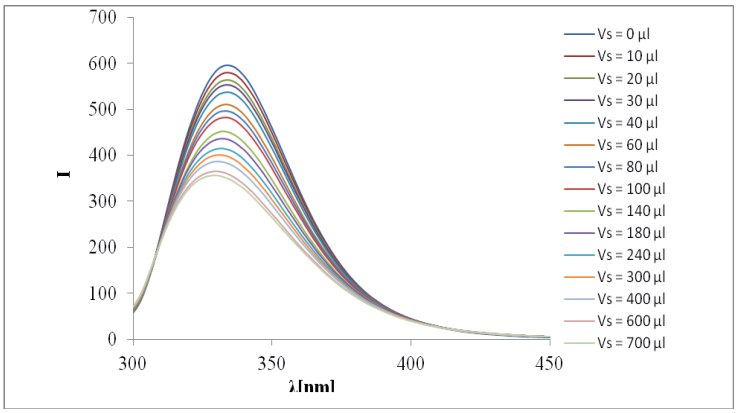

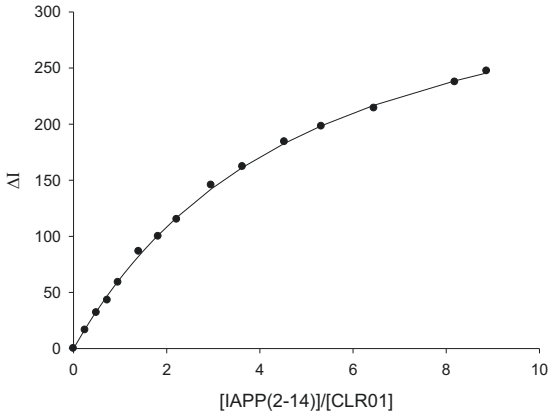

K_a [M^{-1}] = 9540 ± 357 (± 3.7%)
K_d = 104 µM

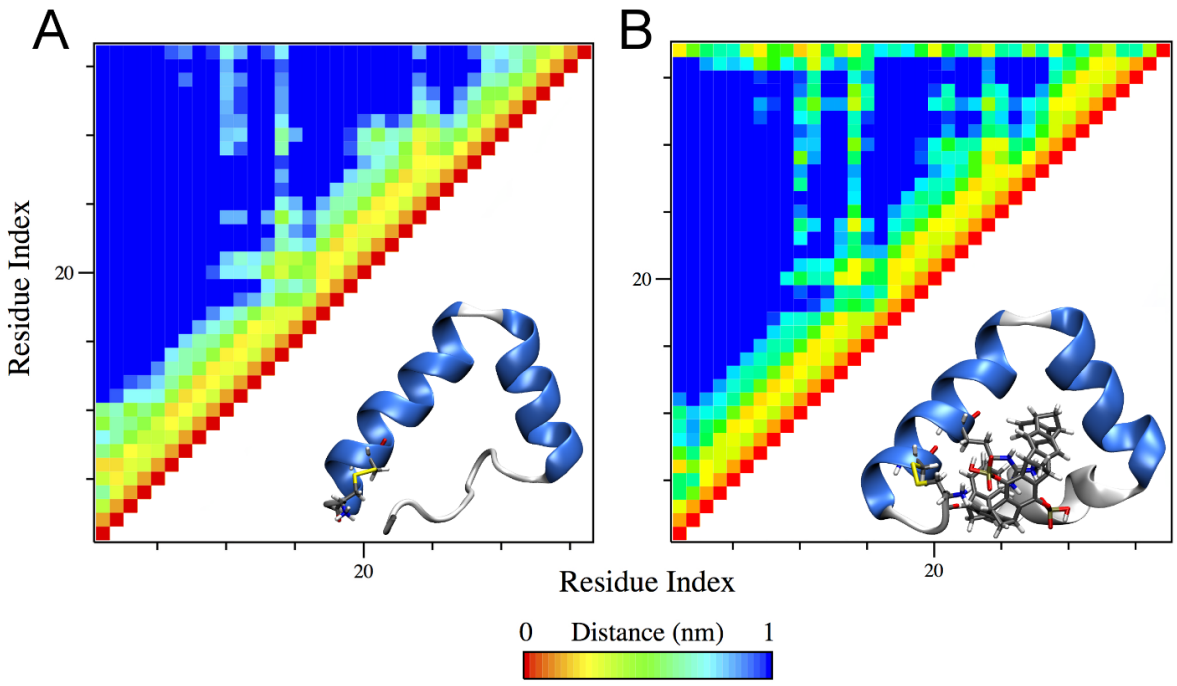

Supplementary Figure S10. Mean smallest distance between residues (contact map) and representative structure of the most populated cluster. A) $IAPP_{2\text{-}37}$, and B) $IAPP_{2\text{-}37}CLR01_{R11}$

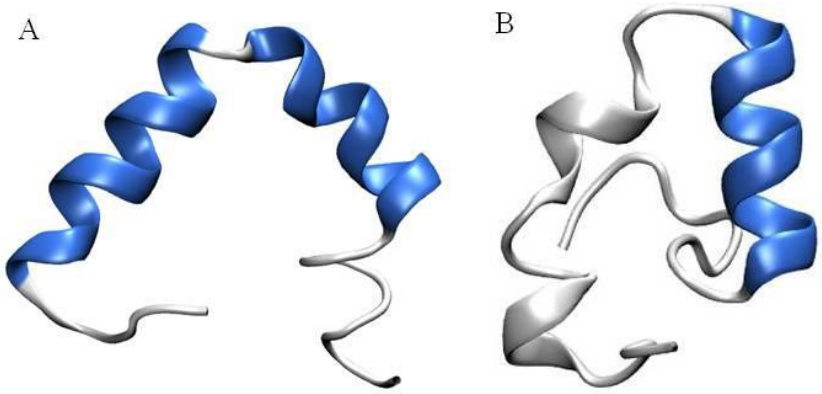

Supplementary Figure S11. Initial geometries of $IAPP_{1\text{-}37}$ in A) $IAPP^{\alpha_{64\%}}_{1\text{-}37}$ (**System I**), B) $IAPP^{\alpha_{27\%}}_{1\text{-}37}$ (**System II**).

Supplementary Table S1. Cluster population analysis: Percent of compact and extended structures

	Kinked	Extended
$IAPP_{1-37}$	4	96
$IAPP_{1-37}CLR01_{K1}$	100	0
$IAPP_{1-37}CLR01_{R11}$	95	5
$IAPP_{1-37}CLR01_{K1+R11}$	100	0
$IAPP_{2-37}$	89	11
$IAPP_{2-37}CLR01_{R11}$	100	0

Supplementary Table S2. Selected geometrical parameters illustrating the inclusion of K1 (left structure) or R11 (right structure) side chains inside the tweezer's cavity. The $C_p - C_p$ and $C_m - C_m$ distances (Å, dotted red lines) indicate the deformation of the tweezers upon inclusion of the amino acids in the cavity. The distance N/C – P (Å) and the corresponding angle (degrees, dotted green lines) indicate how deep the side chains are inside the tweezer cavity. In the case of R11, C is the central carbon atom of the guanidinium moiety.

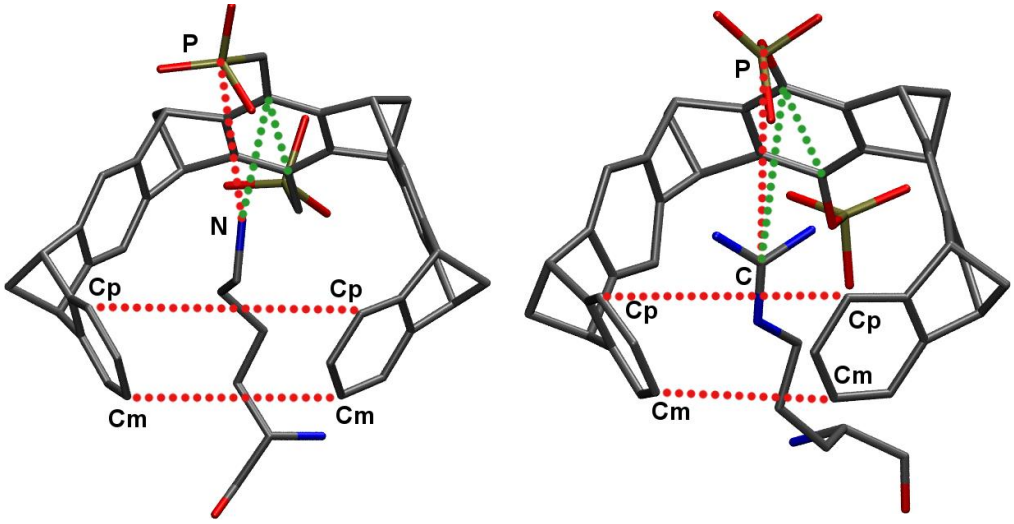

	$C_p - C_p$	*$C_m - C_m$*	*$N(C)^b - P$*	*Angle*
Crystal Structure[a]	5.89	4.20	3.89	90.8
		System I		
$IAPP_{1-37}CLR01_{K1}$	5.59 ± 0.53	4.09 ± 0.55	3.95 ± 0.14	85.9 ± 6.4
$IAPP_{1-37}CLR01_{R11}$	5.80 ± 0.39	4.10 ± 0.42	4.90 ± 0.69	81.6 ± 12.2
$IAPP_{1-37}CLR01_{K1+R11}$	$(5.81 \pm 0.51)_{K1}$	$(4.36 \pm 0.58)_{K1}$	$(4.17 \pm 0.63)_{K1}$	$(90.1 \pm 8.1)_{K1}$
	$(6.37 \pm 0.65)_{R11}$	$(5.06 \pm 0.87)_{R11}$	$(4.70 \pm 0.48)_{R11}$	$(73.9 \pm 11.3)_{R11}$
$IAPP_{2-37}CLR01_{R11}$	5.90 ± 0.37	4.33 ± 0.45	4.61 ± 0.54	77.0 ± 10.9
		System II		
$IAPP_{1-37}CLR01_{K1}$	5.61 ± 0.46	4.15 ± 0.43	3.97 ± 0.26	87.87 ± 7.68

(a) Crystal structure values of CLR01 complexed with K in a 14-3-3 protein (*3*).

(b) N – P distances correspond to CLR01:K complexes and C – P distances to CLR01:R complexes.

Supplementary Table S3: Secondary structure content for selected conformations of $IAPP_{1-37}$ (at t = 0 and t = 10 ns) and averaged over the REMD simulations of $IAPP_{1-37}$ and $IAPP_{1-37}$ $CLR01_{K1}$ in **System II**.

		Helix	Coil	Turn	3-10-helix
System II	$IAPP_{1-37}$ (t = 0)	27.02	32.43	21.62	18.91
	$IAPP_{1-37}$ (t = 10 ns)	45.94	35.13	10.81	8.1
	$IAPP_{1-37}$	63.23	26.11	10.33	0.33
	$IAPP_{1-37}$ $CLR01_{K1}$	59.44	29.72	10.81	0.83

References

1. Rahimi, F., Murakami, K., Summers, J. L., Chen, C. H. B., and Bitan, G. (2009) RNA aptamers generated against oligomeric Aβ40 recognize common amyloid aptatopes with low specificity but high sensitivity, *PLoS One 4*, e7694.
2. Sinha, S., Lopes, D. H., Du, Z., Pang, E. S., Shanmugam, A., Lomakin, A., Talbiersky, P., Tennstaedt, A., McDaniel, K., Bakshi, R., Kuo, P. Y., Ehrmann, M., Benedek, G. B., Loo, J. A., Klärner, F. G., Schrader, T., Wang, C., and Bitan, G. (2011) Lysine-specific molecular tweezers are broad-spectrum inhibitors of assembly and toxicity of amyloid proteins, *J. Am. Chem. Soc. 133*, 16958-16969.
3. Bier, D., Rose, R., Bravo-Rodriguez, K., Bartel, M., Ramirez-Anguita, J. M., Dutt, S., Wilch, C., Klärner, F. G., Sanchez-Garcia, E., Schrader, T., and Ottmann, C. (2013) Molecular tweezers modulate 14-3-3 protein-protein interactions, *Nat. Chem. 5*, 234-239.